semi-infinite system. However, the wavelength of such oscillations is of the order of 6.5 fm, which is much larger than wavelength of the Thrope-Thouless–type oscillations. The two kinds of oscillations are thus quite distinguishable and the two types of calculations can be considered complementary.[8]

Of particular interest is the appearance of the first bump on density distribution long before the regime of nuclear matter is reached. This might be surprising but it is not caused by a mistake in calculation. It corresponds to the first zero of the highest-lying momentum state in the Fermi sea.[4] It agrees with considerations based on a Thomas-Fermi calculation in a linear potential.[9] It is also in agreement with considerations due to diffuseness of the one-body potential.[4] Furthermore, it can also occur in a slab calculation,[3] if the range of the two-body interaction is chosen long enough. However, in this last case the Skyrme-type interaction in Ref. 3 was found not good enough to produce accurate density oscillations, as has already been pointed out.[10]

The author wants to thank Professor M. Baranger for supervision in studying semi-infinite nuclear matter. He also wants to thank Professor J. W. Negele for many discussions.

[1]H. D. Keller, Nucl. Phys. A175, 141 (1971), and references cited therein. For more recent work, see D. G. Ravenhall, C. D. Bennett, and C. J. Pethick, Phys. Rev. Lett. 28, 978 (1972).

[2]B. D. Day, Phys. Rev. 136, B1594 (1964).

[3]P. Bonche, S. Koonin, and J. W. Negele, Phys. Rev. C 13, 1226 (1976).

[4]A. Khakpour, Ph.D. thesis, Massachusetts Institute of Technology, 1975 (unpublished).

[5]D. W. L. Sprung and P. K. Banerjee, Nucl. Phys. A168, 273 (1971).

[6]J. W. Negele, Phys. Rev. C 1, 1260 (1970). See also X. Campi and D. W. L. Sprung, Nucl. Phys. A194, 401 (1972).

[7]M. A. Thorpe and D. J. Thouless, Nucl. Phys. A156, 225 (1970).

[8]R. A. Broglia, A. Molinari, and T. Regge, Ann. Phys. (NY) 97, 289 (1976). See also T. Regge, Low Temp. Phys. 9, 123 (1972).

[9]H. A. Bethe, Phys. Rev. 167, 879 (1968).

[10]J. W. Negele, in Proceedings of the Saclay Meeting on Electron Scattering at Intermediate Energy, Centre d'Etudes Nucleaires de Saclay, France, 1975 (unpublished), and Massachusetts Institute of Technology Center for Theoretical Physics Report No. CTP-505, 1975 (unpublished).

Collective Sideward Flow of Nuclear Matter in Violent High-Energy Heavy-Ion Collisions

Horst Stöcker
Gesellschaft für Schwerionenforschung, D-6100 Darmstadt, Germany

and

Jouchim A. Maruhn and Walter Greiner
Institut für Theoretische Physik der Universität Frankfurt, D-6000 Frankfurt am Main, Germany

(Received 11 December 1979)

Angular and energy distributions of fragments emitted from fast nucleus-nucleus collisions (Ne→U at 250, 400, and 800 MeV/N) are calculated with use of nuclear fluid dynamics. A characteristic dependence of the energy spectra and angular distributions on the impact parameter is predicted. The preferential sideward emission of reaction fragments observed in the calculation for nearly central collisions seems to be supported by recent experimental data.

Sideward emission of nuclear matter was one of the first predictions of fluid-dynamical model calculations of fast nuclear collisions, implying considerable transformation of the incident kinetic energy into compression and heat energy.[1-6] The outflow of matter from the highly compressed "shock" region reflects a large transverse-momentum transfer. Quite early experiments[2,7] supported this hypothesis: Preferential sideward emission of (mainly) α particles was observed in the irradiation of 4π-sr particle-track detectors with light nuclei at $E_{\mathrm{lab}}=0.2$–4.2 GeV/N when selecting nearly central collisions (only azimuthally symmetric many-pronged stars). This was inter-

preted as being due to a strong, sideward-traveling compression wave, called the Mach shock wave.[2,5-7] Additional indications for quasihydrodynamical behavior in fast nuclear collisions seem to be found in various other recent experiments.[8-11]

To investigate some of these phenomena quantitatively, we performed three-dimensional nonrelativistic fluid-dynamical calculations of the collisions of neon projectiles with uranium nuclei at various bombarding energies, a system extensively studied experimentally. The Euler equations were integrated numerically.[4,6] They ensure the conservation of particle number, momentum, and energy. The important input to these equations is the nuclear equation of state, i.e., the functional dependence of the internal energy $W(\rho,T)=E-E_{\mathrm{kin}}$ and the pressure $p=\rho^2(\partial W/\partial\rho)_s$ (at constant entropy s) on the local density ρ and temperature T. $W(\rho,T)$ is split into the compression energy $E_c(\rho,T=0)$ and the thermal energy $E_T(\rho,T)$. For $E_c(\rho)$ a parabolic expansion around the ground-state density with a compression constant $K=200$ MeV and for $E_T(\rho,T)$ a Fermi-gas *Ansatz* is used.[1,2,6] The Coulomb and Yukawa potentials are treated explicitly.[6] They allow for a realistic treatment of the binding and surface energies of the nuclei. However, it must be emphasized that the reaction dynamics is practically not influenced by the Coulomb and Yukawa forces at high collision energies ($E_{\mathrm{lab}}\sim 400$ MeV/N): We find that they are only important for the stability of the incident nuclei. The evolution of the system is followed in time and the energy spectra and angular distributions are calculated by integrating the matter flux over all space. The computation is stopped at a late stage when the compressed matter has expanded so that the maximum density is less than $\rho_s\sim 0.5\rho_0$, where thermal contact between the nucleons becomes questionable because of their large distances. The final spectra and angular distributions were checked to be independent of the exact value of ρ_s.

Figure 1 shows snapshots of the density and temperature contours and of the velocity field in the scattering plane in a late stage of the reaction Ne + U at $E_{\mathrm{lab}}=400$ MeV/N for two different impact parameters $b=0$ and 6 fm. For head-on collisions [Fig. 1(a)] two zones can be distinguished: Near the collision axis, where the projectile directly hits the target, a strongly compressed, highly excited head shock is formed. In contrast to the oversimplified geometrical "fireball" models, the head shock pushes matter

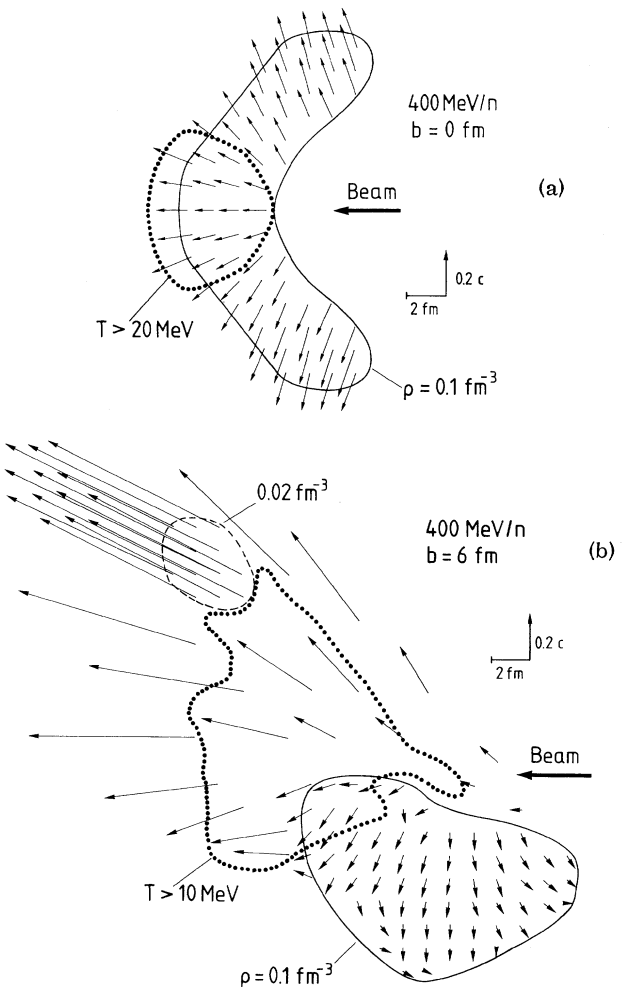

FIG. 1. Density and temperature contours and velocity field (arrows) in the scattering plane at a late stage of the reaction. (a) Central collision; (b) Intermediate impact parameter.

sidewards, thus initiating a strong, sideward-traveling compression wave (called shock[2]). The small velocities everywhere are remarkable: No projectilelike fragments are observed; the forward momentum is transferred to the combined target-plus-projectile matter. The angular distribution of emitted fragments shown in Fig. 2(a) is sidewards peaked at the Mach-shock-wave angle $\theta_{\mathrm{MS}}\approx 70°$. Most of the contribution to the peak arises from particles with small kinetic energies $E_{\mathrm{kin}}=20\pm 10$ MeV (dashed line) and these also dominate the energy distribution [Fig. 2(b)]. Practically no fast particles can be seen. It should be stressed, though, that the locations of the maxima in the angular distributions and energy spectra are not well determined because of

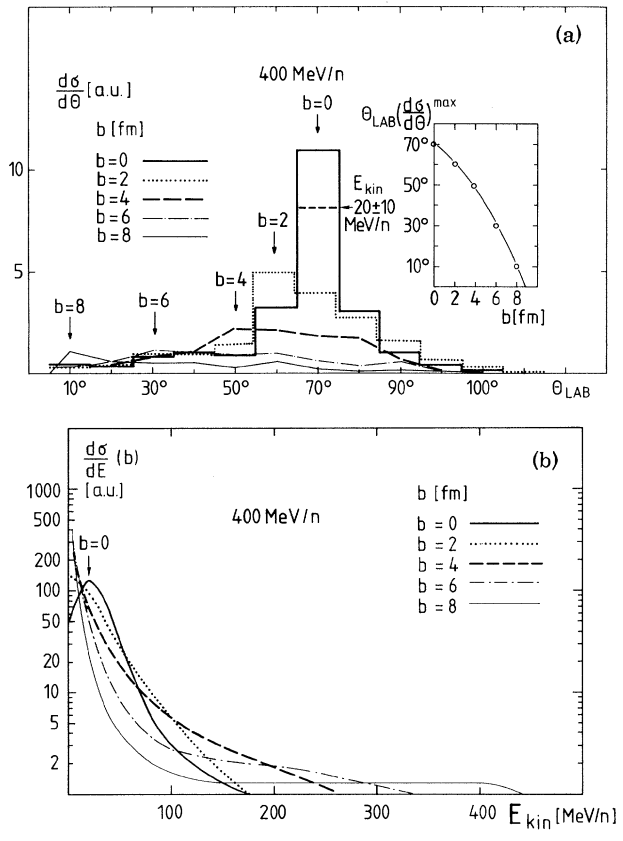

FIG. 2. Impact-parameter dependence of (a) angular distribution (inset: position of maximum), and (b) energy spectra of reaction products.

the rather poor statistics characteristic of hydrodynamic-type calculations.[4,6] Also, only the sharp peak in $d\sigma/d\theta$ of Fig. 2(a) at $b=0$ corresponds to a peak in $d\sigma/d\Omega$, whereas in the double-differential cross section $d^2\sigma/d\Omega\, dE$ peaks appear even for $b\neq 0$, as is the case for the experimentally observed peaks in Ref. 9.

In nearly central collisions the maximum of the cross section is still located at small forward and small perpendicular momenta $p/M \lesssim 0.2$ close to the target rapidity. Forward emission is suppressed. For collisions of equal nuclei the sideward emission is seen at forward angles in the laboratory system though mainly with large kinetic energies (above the center-of-mass energy).[6] In Fig. 1(b) the analogous situation is shown for $b=6$ fm. Here two nuclear residues are kicked apart by the highly compressed head shock zone ("bounceoff" effect[6]). The velocity field shows that the target residue slowly moves to $\theta_{lab} \approx 90°$ and is expected to fission because of its large deformation and angular momentum. The projectile residue is deflected to forward angles ($\theta_{lab} \approx 30°$) and is azimuthally anticorrelated with the target residue.

The two kinds of events just presented—the Mach shock wave for nearly central collisions and bounceoff for the intermediate impact parameters—can be distinguished by their characteristic dependence of the calculated fragment angular distributions and energy spectra on the impact parameter [see Figs. 2(a) and 2(b)]. For increasing impact parameter, the angular distributions broaden. The maxima of $d\sigma/d\theta$ corresponding to the deflected projectile fragments shift to smaller angles [see the inset to Fig. 2(a)]. The contribution of the high-energy tails of the spectra (up to the incident energy) increases with b. This increase is partly due to the deflected projectile residue, and partly to the exploding head-shock matter. Low-energy particles with $E_{kin} \lesssim 5$ MeV/N coming mostly from the target residue dominate for intermediate b. For $b=8$ fm, two distinct contributions are observed in the matter distribution, one arising from the bounced-off projectilelike fragments at large transverse and forward momenta, the second bigger one from the residual target at low parallel and perpendicular momentum (i.e., near the target's initial position).

For $b=4$ and 6 fm, the double-differential cross sections show an important feature (see Fig. 3): There are maxima in the angular distributions that move to forward angles with increasing fragment kinetic energy [see Fig. 3(c)]. At $b \lesssim 4$ fm, the broad low-energy backward peak caused by the shock wave is much higher than the narrow forward peak in the medium kinetic-energy windows.

Experimental evidence for the bounce-off effect in intermediate-impact-parameter collisions was found[9]: In Ne + Au reactions slow heavy-target residues, moving to 90° in the laboratory system, were detected in coincidence with 180° azimuthally correlated jets of fast, light particles, which can be attributed to the bounced-off projectile matter. To investigate the nearly central collisions, Stock *et al.* selected events with high multiplicities in Ne + U collisions.[10] For an estimated mean impact parameter of $\bar{b} \approx 4$ fm, they find maxima in the proton angular distributions. The low-energy particles show a broad 90°-peaked distribution, which becomes narrower and shifts to forward angles with increasing kinetic energy, in qualitative agreement with the results presented here. One

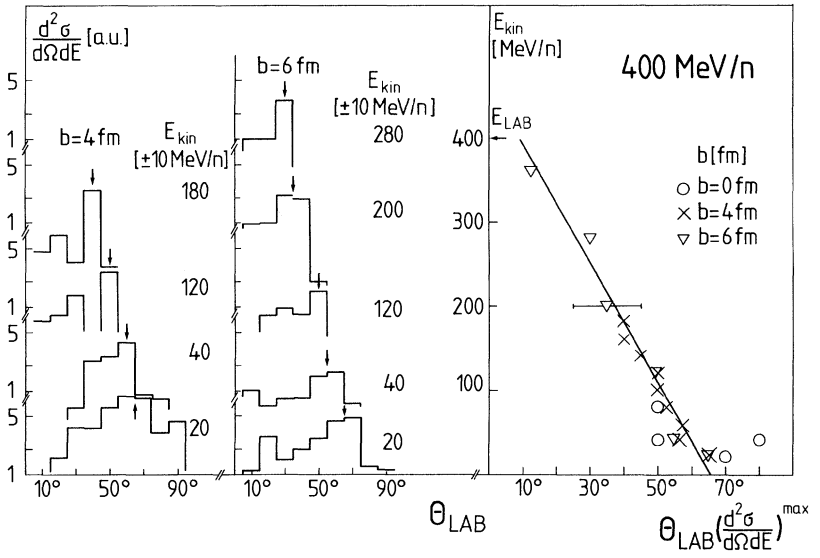

FIG. 3. Double-differential cross section, plotted as angular distributions for different fragment kinetic energies, for 4- and 6-fm impact parameters. The right-hand-side plot shows the position of the maximum as a function of the laboratory angle.

interesting possibility is the search for superdense abnormal states of nuclear matter via irregularities in the excitation function of the Mach–shock-wave angle[5] $\theta_{MS}(E_{1ab})$ and of other measurable quantities (pion production rate, temperature, etc.).[6]

In conclusion we have discussed strong-compression phenomena in violent nucleus-nucleus collisions in nuclear fluid dynamics. We find predominant sideward emission of matter for small impact parameters. The characteristic features of the recent experimental data seems to support the theoretical results. Additional theoretical and experimental efforts are necessary, however, to extract conclusive information on the properties of dense nuclear matter from these phenomena.

This work was supported by the Bundesministerium für Forschung und Technologie (BMFT).

[1]W. Scheid, H. Müller, and W. Greiner, Phys. Rev. Lett. 32, 741 (1974); J. Hofmann, W. Scheid, and W. Greiner, Nuovo Cimento 33A, 343 (1976).

[2]H. G. Baumgardt *et al.*, Z. Phys. A 237, 359 (1975).

[3]A. E. Glassgold, W. Heckrotte, and K. M. Watson, Ann. Phys. (N. Y.) 6, 1 (1959); G. F. Chapline, M. H. Johnson, E. Teller, and M. Weiss, Phys. Rev. D 8, 4302 (1973); M. I. Sobel, P. J. Siemens, J. P. Bondorf, and H. A. Bethe, Nucl. Phys. A251, 502 (1975).

[4]C. Y. Wong and T. A. Welton, Phys. Lett. 49B, 243 (1974); C. Y. Wong, J. Maruhn, and T. A. Welton, Nucl. Phys. A253, 469 (1975); A. A. Amsden, G. F. Bertsch, F. H. Harlow, and J. R. Nix, Phys. Rev. Lett. 35, 905 (1975), and Phys. Rev. C 17, 2080 (1978); H. Tang and C. Y. Wong, to be published.

[5]J. Hofmann, H. Stöcker, U. Heinz, W. Scheid, and W. Greiner, Phys. Rev. Lett. 36, 88 (1976).

[6]H. Stöcker, J. A. Maruhn, and W. Greiner, Z. Phys. A 290, 297 (1979), and 293, 173 (1979), and Phys. Lett. 81B, 303 (1979).

[7]E. Schopper and H. G. Baumgardt, J. Phys. G 5, 231 (1979).

[8]K. L. Wolf *et al.*, Phys. Rev. Lett. 42, 1448 (1979); A. Sandoval *et al.*, Lawrence Berkeley Laboratory Report No. LBL-8771, 1979 (to be published).

[9]W. G. Meyer, H. H. Gutbrod, Ch. Lukner, and A. Sandoval, Lawrence Berkeley Laboratory Report No. LBL-9151, 1979 (to be published).

[10]R. Stock *et al.*, Gesellschaft für Schwerionforschung, Darmstadt, Report No. GSI-22-79, 1979 (to be published).

[11]A. A. Antonenko *et al.*, Pis'ma Zh. Eksp. Teor. Fiz 28, 609 (1978) [JETP Lett. 28, 561 (1978)], and to be published.